

Density distribution configuration and development of vortical patterns in accreting close binary star system

Daniela Boneva, Lachezar Filipov

Space Research and Technology Institute, Bulgarian Academy of Sciences,
danvasan@space.bas.bg, lfilipov@space.bas.bg

October 11, 2012

Abstract

We investigate the problem of structures formation in accretion disc zone, resulting from the tidally interaction in close binary star system. We aim to examine the area where the incoming flow meets the matter around secondary star and the resulting effects throughout the accretion disc. The research is based on employment of the fluid dynamics equations in conjunction with numerical simulations leading to the design of graphical models of accretion processes. For the simulation we propose box-framed sharing schemes. (i) The tidal transfer of matter through the inner Lagrangian point in close binary stars disturbs the flow in discs zones and outer disc area. Calculations on the perturbed parameters of density and velocity reveal formation of a thickened zone in the contact area of interacted flows. It appears to be stable for a number of periods and is unaffected by rotation and dissipation processes. (ii) The results also show development of undulations, which grow to vortical patterns in the accretion disc's zone. It is confirmed that under the influence of tidal wave the conditions of reconfiguring of accretion flow structure are generated.

Keywords: Accretion; accretion disks; Hydrodynamics; Waves; Methods: numerical; (Stars): binaries: close;

1 Introduction

Study of the flow structure in astrophysics is important, because the results could be used both for consideration of the evolution status of binary stars and for the interpretation of observational data. Therefore, when investigating close components, it is necessary to include physical essence of the flow dynamics response to the interaction processes. In the astrophysics of binary stars, one of the most investigated phenomena are vortexes. Vortices and spiral configurations play a key role in the accretion disc dynamics, because they are considered as an efficient mechanism of angular momentum transportation (Baranco & Marcus 2005) in regions where the magneto-rotational instability (Balbus & Hawly 1998) does not operate. At present, there are many hydrodynamics studies in finding the way of vortices appear and behave in the flow. Li et al. (2000, 2001) have shown that vortices are formed by Rossby waves instability and moving radially and thus transport mass through the disc. Vortices can be generated by a globally unstable radial entropy gradient (Klahr & Bodenheimer 2003) that may result in local outward transport of angular momentum. In astrophysics, the problems of structures development have been investigated mainly numerically (e.g. Lithwick 2009; Godon & Livio 1999). Bracco et al. (1998) by using two-dimensional, incompressible fluid dynamics, show that anticyclonic vortices shift out and that smaller vortices merge

to form larger vortices. Godon & Livio (1999, 2000) confirm this result with two-dimensional, compressible, barotropic simulations. Shen et al. (2006) examine the formation of 2D vortices starting from 2D turbulence in fully compressible simulations. Barranco & Marcus (2005) compute the evolution of 3D vortices and show that part of the vortical formations could be destroyed, but the other part survive for several hundreds of orbits. They use an "inelastic code" with vertical stratification and examine the influence of 3D perturbations over the vortices in the middle disc's zone. By performing a series of runs with zero initial vorticity and perturbation wavelengths, Johnson and Gammie (2006) give a very realistic way of the initial vorticity generation. They have noted that the remaining vorticity can be generated from "finite-amplitude compressive perturbations". Johnson and Gammie (2005) argue that the vortices are "long-lived" assuming they could not be conserved in 3D calculations. Lesur and Papaloizou (2009) have obtained that most anticyclonic vortices are unstable. Their simulations show that only the vortex core is stable and that the instability appears at the vortex boundary. Formation of vortices could be accompanied with spirals and vice-versa. Fridman (2007) confirms that for one arm spiral waves in the disc, based on the spiral wave theory. Sawada, in his paper (Sawada et al. 1986), finds that a two-armed spiral structure developed in the result of 2-D simulations of mass transfer via Roche lobe overflow. Their research has been followed by a series of investigations (e.g. Rozyczka & Spruit 1993), finding that during the stage of spirals development the appearance of vortices are observed, after the interaction event. In our previous studies we have found that presence of one-armed spiral structure could be arisen as an effect of tidal interaction of two stars in binary system (Boneva 2010(1), Boneva 2010(2)). The same spiral wave structures are observed in the calculations of (Bisikalo et al 2008; Steeghs et al. 1997). Currently, the question of how the structures in accretion discs arise is still open for discussion, along with numerous unresolved problems concerning the formation mechanism and the duration of vortices existence in discs. By applying numerical calculations on gas-dynamical flow, we suggest modeling of patterns formation and explanation of supporting physical processes in interacting flows. The paper is organized as follows: Section 2 presents some base equations and the methods of analysis on it. In Section 3 we introduce the main results that reveal the variations in disc's and vicinity's density. The development of vortical structures formation is examined and described in Section 4.

2 Basic equations and methods

2.1 Basic equations

The nature of the interaction between a flow of matter and an envelope of two star components requires employment of gas-dynamics equations. Therefore, to obtain solutions of the above stated problem a system of equations is needed. Herein, the basic equations are presented in a form that have been suggested and affirmed by many authors: (Shore 2007; Clark & Carswell 2007; Frank et al. 2002; Graham 2001; Shu 1992).

We present the equations in their vector form. The equation of mass conservation is:

$$\frac{\partial \rho}{\partial t} + \nabla \cdot (\rho v) = 0; \quad (1)$$

The existence of viscous processes in the accretion flow, as well as influence of forces and rotation could be performed by the following useful form of the Navier-Stokes equations, suggested by (Thorn 2004) and simplified here:

$$\frac{\partial v}{\partial t} + v \cdot \nabla v = -\frac{1}{\rho} \nabla P - \Omega \times (\Omega \times r) - 2\Omega \times v - \nabla \Phi + \nu \nabla^2 v \quad (2)$$

Where the basic notations are: ρ is the mass density of the flow, v - is the velocity of the flow; P - is the pressure; ν - is the kinematic viscosity; Ω - is the angular velocity; $\Omega \times (\Omega \times r)$ - is the centrifugal acceleration of the centrifugal force; and $2\Omega \times v$ - is the Coriolis acceleration in the mean of the Coriolis force. In the current analysis $\rho \neq \text{const}$ and $\nu \neq 0$. Φ is the gravitational potential and it depends on the density distribution inside each of the star's component (Boyarchuk et al. 2002). Then the gravitational potentials Φ_1 and Φ_2 could be defined from the Poisson's equations: $\Delta\Phi_1 = 4\pi G\rho_1$ and $\Delta\Phi_2 = 4\pi G\rho_2$

The energy balance equation for a viscous non-ideal fluid is:

$$\frac{\partial}{\partial t} \left[\rho \left(\frac{1}{2}v^2 + \varepsilon + \Phi \right) \right] + \nabla \cdot \left[\rho v \left(\frac{1}{2}v^2 + h + \Phi \right) - 2\eta\sigma.v \right] = 0; \quad (3)$$

Where $\frac{\partial}{\partial t} \left[\rho \left(\frac{1}{2}v^2 + \varepsilon + \Phi \right) \right]$ is the total energy density, where the first term on the left denotes the kinetic energy, the second is the internal energy and the third expresses again the full potential of the gravitational fields.

And $\left[\rho v \left(\frac{1}{2}v^2 + h + \Phi \right) \right]$ is the total energy flux, where $h = \varepsilon + P/\rho$ is the enthalpy, η is the shear (or dynamical) viscosity of the flow, and σ is the rate of shear.

The equation of state for compressible flow is:

$$P = c_s^2 \rho \quad (4)$$

where c_s is the sound speed.

We present the equations in the above system in their common form and we can easily transform them into quantities for each of the posted problems.

Next to explore is the vortical transport equation, because it is related to the examination of transfer's mechanisms in the flow. This equation could be derived in the following commonly used way, how it has been done by Nauta (2000), Lithwick (2007), Godon (1997). If the curl of Navier-Stokes equations is considered, and use the expressions: $\Psi = \nabla \times v$ - expressing the vorticity in the flow; $(v \cdot \nabla) v = \nabla \frac{v^2}{2} - (v \times \Psi)$ and $\left(\frac{\partial \Psi}{\partial t} + v \cdot \nabla \right) \frac{1}{\rho} = \frac{\nabla \rho \times \nabla P}{\rho^3}$; then the following expression is obtained:

$$\frac{\partial \Psi}{\partial t} + \Psi (\nabla \cdot v) + (v \cdot \nabla) \Psi = - \frac{\nabla p \times \nabla \rho}{\rho^2} + D \nabla^2 \Psi \quad (5)$$

Here Ψ - is the vorticity; D - is the diffusion coefficient (or matrix of the transport coefficient).

This equation expresses the relation between the transport coefficient, which takes part in the angular momentum transfer, evolution of the vorticity with time and the non-convective relationship between density and pressure in the flow. Non-conservancy of specific vorticity by the each fluid element is observed in the right-hand side of Eq. (5), which gives a condition for baroclinicity in the flow (Lovelace et al. 1999), and enables the development of vortices in the accretion matter. The baroclinicity of the general flow is given by the baroclinic term (Klahr 2004; Petersen 2007): $\nabla \rho(r, z, \varphi) \times \nabla p(r, z, \varphi) \neq 0$. The importance for this instability is the non-axisymmetric deviations from the mean state which can lead to the rise of the baroclinic term even in two dimensions: $\nabla \rho(r, \varphi) \times \nabla p(r, \varphi) \neq 0$ and vorticity can be generated. This instability, known as baroclinic (Klahr & Bodenheimer 2000, 2003) and arising vortices are discussed in Section 4 of the current survey.

2.2 Numerical methods

The complexity of the studied problem and analysis on the corresponding equations in hydrodynamical matter, require applying of numerical codes. We use "PDEtools" and "PDEsolve" packages, implicated in Maple 5 and Maple 12 (Maple Tutorials of Monnagan et al. 1998; Heal et al. 1998). We chose to insert into calculations the methods, which are employed in these codes, known as: the Runge-Kutta (implicit part) method (further referred to as RK), Alternating direction implicit method (ADI), CenteredTime1Space(CTS)[forward/backward], BackwardTime1Space(BTS)[forward/backward], based on finite difference scheme or Godunov's algorithm. More detail description for RK and ADI methods could be found in (Autar & Egwu 2008; Chang et al. 1991) and in Maple Tutorials again for CTS and BTS. All they are implicit methods, which are general in their application. It is suitable to use them in the solutions of partial differential equations, because of their high stability. We give here a short description of their operation.

The method of Runge-Kutta is widely used in physical calculations. The method treats every step in a sequence of steps in identical manner. That fact makes it easy to add in Runge-Kutta into relatively simple schemes (Forsythe et al. 1977). This is mathematically proper, since any point along the trajectory of an ordinary differential equation can serve as an initial point.

Euler method is a part of RK family methods and it's common expression is: $y_{n+1} = y_n + hf(x_n, y_n)$, which is unsymmetrical. It advances the solution through an interval h , from x_n to $x_{n+1} = x_n + h$ and uses derivative information only at the beginning of that interval. This means that the step's error is only one power of h smaller than the correction, i.e. the member $O(h^2)$ is added to that expression.

The symmetrization in the error term could cancels out the first-order error term, making the method second order. (If the error term of the method is $O(h^{n+1})$, a method is known as n -th order). Adding up the right combination of these, we can eliminate the error terms order by order (Cash & Karp 1990). That is the basic idea of the Runge-Kutta method and we applied its schemes to equations posted in the current survey.

It is common that numerical codes need some control during the processing. Adaptive step-size control is used here (Cash & Karp 1990; Hairer & Soderling 2005), with the purpose of achieving some predetermined correctness in the solution with minimum computational effort. Implementation of adaptive step-size control requires that the stepping algorithm returns information about its performance and estimation of its truncation error.

ADI method belongs to the group of finite difference methods and follows the idea to split the finite difference equations in two, in relation to the derivatives in coordinates taken implicitly. The system of equations then becomes symmetric and tridiagonal and is usually solved with tridiagonal matrix solver.

The centered time forward/backward space method and backward time forward/backward space method are implicit single stage methods that can be used to find solutions to PDEs containing the derivatives $v, v[x], v[t], v[xt]$. In the both methods, PDEs that describe right-traveling waves should use the backward method (specified as [backward]), and specify the boundary condition at the left boundary, while left-traveling waves require the forward method (specified as [forward]), and the boundary condition at the right boundary. Numerical boundary conditions are not required. The points of discretization that are used to compute the values of the grid are different: $(t+k, x[i])$ is in BTS; $(t+k/2, x[i])$ in CTS.

We test the equations with the "pctest" tool, which checks if the solution is correct. To reduce the PDEs to a simpler problem, we applied an "ansatz" tool. The specifying initial and boundary conditions are assigned in Sects. 3 and 4 in accordance with the presented model. Box-framed scheme has been suggested and applied. We could perform the calculations in limited regions of all

disc's areas by configuring the scheme for each problem, Then, we make the calculations inside of the box, or frame with different measurement. We have made the code validation, applying it to the problem of shock wave distribution in a tube. The box-framed model has been applied again.

2.2.1 Image resolving and processing methods

We depict most of the results by graphic simulations, which present some full picture of the studied processes. Then, based on the images decipherment, we have to identify the fine forms for better interpretations of the results. For the purpose of the study the high-pass: Gaussian filters, which are adequate to enhance the structure of the graphical results and to obtain spatial filtered image (Gonzalez & Woods 1992), are applied. They can be used to enhance edges between different regions. The Gaussian filters are part of Convolution filters which remove the low frequency components of an image while retaining the high frequency (Haddad & Akansu 1991, Shapiro & Stockman 2001) local variations. This is accomplished using a kernel with a high central value, typically surrounded by negative weights. High pass filter with $[3 \times 3]$ kernel is used with a value of 8 for the central pixel and values of -1 for the exterior pixels; high pass filters can only have odd kernel dimensions. We employ this method in Section 4.

The convolution filters produce output images in which the brightness value at a given pixel is a function of some weighted average of the brightness of the surrounding pixels. Convolution with the image array returns a new, spatially filtered image (Nixon & Aguado 2008). Different types of filters can be generated by selecting the kernel size and values, producing (Vandevenne 2004-2007).

We have found the above combination of methods suitable for the exploring here processes: mass transfer, interaction of the flows and concomitant structures formation. Application of these methods and results are presented in the next two sections. All used equations from Sect. 2.1 are transformed further in cylindrical frame of reference (r, φ, z) . This system allows applying 2D and 3D numerical modeling of structure of the flowing matter. The modeling is performed in non-inertial frame of reference and quadratic 2D - 3D set.

3 Disturbances in the flow density and velocity. Formation of "thickened zone".

The gas-dynamical analysis of the flow structure in the close binary star system has revealed tidal interaction between the out-flowing matters from donor through the point of libration L_1 and the flow around the accretor (Boyarchuk et al. 2002; Bisikalo et al. 2003; Frank 2008; Pringle 1985, 1992). Bisikalo et al. (2001) have shown that even a small variation in mass transfer rate of the binary system, could disturb the equilibrium state of the hot accretion disc. This may cause the appearance of area with increased density, called "blob". Using this result as a point, we obtained a similar dense formation, called "thickened zone". We used the above numerical methods in the calculations (RK & ADI) and reported the solution in paper Boneva (2010) firstly. The graphical result there was obtained only for a moment of time in one period of rotation to mean an orbital period: $\sim t_{m0} + 0.25P_p$ (see Fig.1a and Fig. 6 in Appx.). Where t_{m0} denotes the moment of time when the mass transfer rate begins to change and P_p is the orbital period of the binary system. In the current study, the simulations are performed for three additional moments of rotational period, until one orbital period of the system is fulfilled, see Fig. 1 (b), (c), (d): $\sim t_{m0}; +0.57P_p; +0.78P_p; +0.92P_p$. We repeated numerical runs for $\sim 4.5P_p$.

We apply free boundary conditions at the outer disc edge, where the density is defined to be constant: $\rho_{out} = 10^{-8}\rho_{L_1}$, where ρ_{L_1} is the density of the inner Lagrangian point L_1 . In the inner regions, where the mass transfer and the interaction of streams take place, the values of the

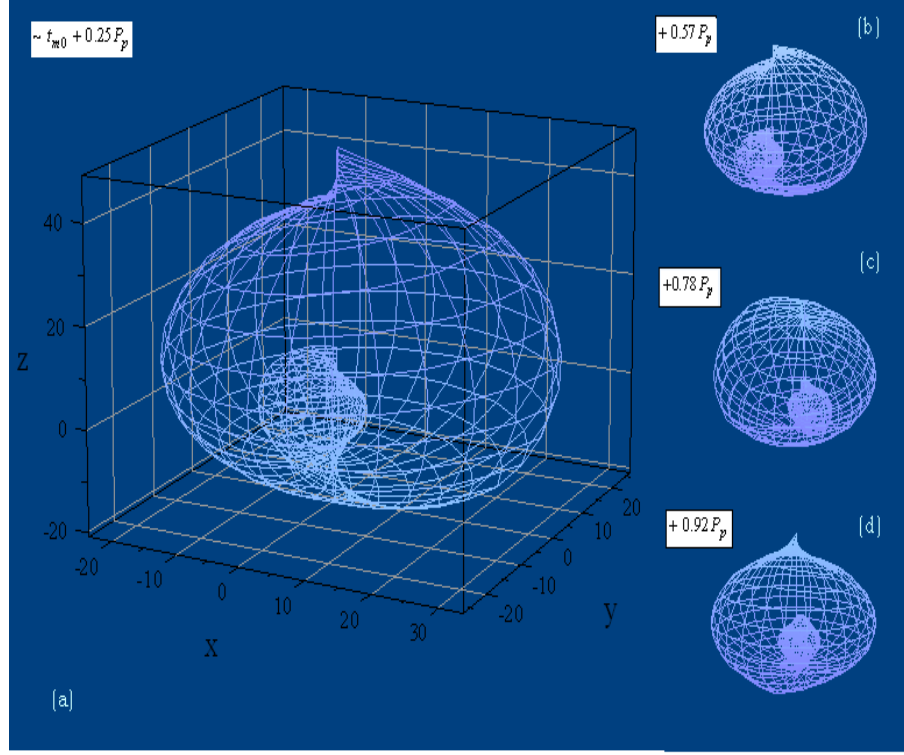


Figure 1: Thickened zone formation, as a result of disturbances in the stability state, caused by mass transfer in a binary system. The whole system consecutive phases of rotation can be seen in four images (a), (b), (c), (d). The dense pattern, colored in light blue, is observed in all phases at the image. The detection's stop-steps of one rotational period: $\sim t_{m0} + 0.25P_p$; $\sim t_{m0} + 0.57P_p$, $+0.78P_p$, $+0.92P_p$. The mesh grid was taken in a (x, y, z) calculation frame of coordinates, corresponded to the density distribution in r direction over the time t[days].

density, as was shown, could not remain constant. A spherical form of the location of interaction was adopted, with a free radius. The limitations of the software imposed some employment restrictions and shortening the necessary time for these calculations, but it does not affect the final results.

The results show that the thickened zone could exist for a long period of time and it does not change its mean characteristics over the time of our calculations. This is close to the result, reported by Bisikalo et al. (2001) who have showed this for several tens of orbital periods of the binary star system. In the current paper, we stopped our examinations before the mass transfer rate begins to subside.

In the next calculations, we can see that the changes in the mass transfer rate are in a close relation both with disturbances in the density and in the velocity. We put values to the rate of accretion ranging: $\dot{M}_0 \approx 10^{-10} \dot{M}_o/\text{year} \div \dot{M}_{t_0+n} \approx 10^{-12} \dot{M}_o/\text{year}$. To study this, we apply the modified perturbation function, described in Appendix and in (Boneva 2009), on the Navier-Stokes equations (Eq. 2), and obtain the “term of instability”: $\Omega \left(\frac{\partial r^2}{\partial r} \frac{V_r}{r} - \frac{\partial V_\varphi}{\partial \varphi} \right)$. This term gives the relation of velocities, including perturbation value and angular velocity. In this expression $V(r, \varphi)$ is the full quantity of velocity, which is a sum of the perturbation value and the time averaged velocity (see App., Eq. A1). The behavior of perturbed velocity is calculated for different values of the dimensionless parameter m , which is the mode number along φ direction (see Appendix). After the calculations, we detected sharp decreasing in velocity values and it is showed in Fig. 5 (in the

Appx.) and in Boneva (2009). Let's see, how the appearance of our thickened zone is provoked, related to the variability in density and velocity. In the places where the velocity values are close to their minimum, the density starts to increase and it pulls a matter there. Thereafter, this means that the matter from a disc could be pumped out or concentrated within given places, causing the density's dilution in close areas. We express this graphically and the thickening place in the disc can be viewed now in form of the pillar (see Fig.2). The result points for three periods of rotation.

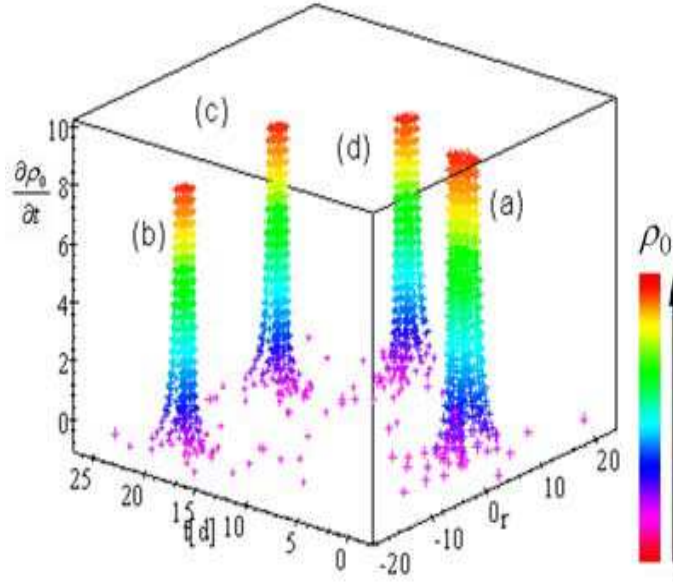


Figure 2: Pillar's form graphical expression of density concentration in close area. The image shows the accumulating matter in four moments of time in a rotational period. Calculations are made in 3D quadratic frame in x, y and on variations of the perturbed density value ρ' .

The pillars, seen in Fig. 2, indicate matter accumulation in the places with increasing density, defined by the boundary conditions area, for several periods of rotation. The image in Fig.2 corresponds to the appearance of dense zone in Fig.1. This result is the second stage of the case presented by Boneva (2010).

4 Development of vortices in the disc flow.

It was already mentioned in Sect. I and it is confirmed by many studies vortices play a vital role in accretion disc dynamics. They are considered to be an effective mechanism of angular momentum transport (Barranco & Marcus 2005). Herein, we perform a computational analysis to reveal one possible way of their appearance by visual simulation of their development in the flow. Our calculations are based on the vortical transport equation (Eq. 5), because it includes the condition that could provokes baroclinic character of the flow, (Klahr & Bodenheimer 2003). The box-frame model is used once again. The introduced boundary conditions are of Dirichlet- and Cauchy type: $r_{v(1+n)} = K(x, y) - \frac{\partial K}{\partial r_v} \frac{\partial}{\partial t}$; $r_{v0}(0) = 0$ is the radius of the vortex; $K(x, y)$ is the boundary area of equations activity. We place the cylindrical coordinates (r, φ, z) frame for the equations and quadratic (x, y) set for the numerical scheme. We perform a series of runs with zero initial

vorticity, but different from zero the initial turbulence values: $v(0) = v_0$, $\Psi_{r,\varphi}(t_0) = 0$, $\rho(t_0) = \rho_0 \approx 2.5 \times 10^{-6} \text{ kg/m}^{-3}$, $t_0 \approx 1$, and $r_0 \approx 1$. Results of the simulations show a vortex type growth in r, φ plane of the disc zone. The box-frame values range from about $7.687 \times 10^{-7} \text{ AU}$ to $6.68 \times 10^{-7} \text{ AU}$ and from $7.687 \times 10^{-8} \text{ AU}$ to $6.68 \times 10^{-8} \text{ AU}$, corresponding to the above values of x and y , referred to as x_b and y_b . The development of this kind of vortices passes through three stages, resulting from the calculations. Firstly, a distortion of the flow laminarity is observed (Fig. 3a). In the next series of calculations, the velocity values step to $(v(t_1, t_{n-1}) \approx v_0 + v_1)$ and the layers in the examined area undergo a weak undulation (Fig. 3b). This means that the variations of velocity and density have significant impact on the flow's behavior. For the final round of calculations the density and velocity accepted values $\rho(t_n), v(t_n)$ are used as an input. Then, we consider the stage of vortex evolution in some steady period of their development, when they are "ready" for the angular momentum transport (Fig. 3c). In contrast to Sect. 3, where it was shown that the thickening patterns are formed inside the disc area, here in this case the development of vortices is more frequently observed along the outer sides, close to the disc's edges. In conclusion, we suppose that, when this kind of vortical formations leave the disc zone, they could crumble and merge into the matter of the circumdisc halo, influenced by the conditions of low density there. The solution of the last assumption is still under investigation and the results will be presented in another report.

We have received the view of the Fig. 3 by image processing stages shown in Fig. 4. Figure 4a shows contour profile of vortex obtained by the result of numerical simulations, which we already described in this section. We apply on it the convolution method by high pass Gaussian filter, discussed in Sect. 2.2.2, and then depict the same vortexes in Fig. 4b. The final model is obtained by removing the outliers and eliminating the inessential elements from the image map (Fig. 4c). We made this in an attempt to better understand the results of these simulations and distinguish the main structure components. The image map gives a summary of the data, including the set of projection of all examined parameters; each pixel of the image consists of some information about the numerical graphical simulations.

The baroclinicity conditions of (Klahr & Bodenheimer 2003), misalignment of pressure gradient and density gradient is required wherever there is azimuthal density gradient. This misalignment acts as a source term for the generation of vorticity in the region of outer edge of the disc. The latter processes have initially been presented in a similar way by Boneva & Filipov (2009) and Boneva (2010), where the received images are of an isolated vortex, which is a part of the examined region, defined above. These vortices may propagate throughout the disc, according to the baroclinicity global character, but they are local, temporal formations. How long these vortices would live and what would destroy them is another unanswered question and unresolved problem. The point we want to make is that two-dimensional simulations have been used to identify physical processes that would likely play a role in a full three-dimensional simulation. If vortices primarily form on the upper and lower surfaces of accretion discs, then the radiative cooling rates could be rapid, as was shown in the numerical results by Barranco & Marcus (2005). Therefore, it could be expected that vortices confined to the surface of a disc could have longer lifetimes due to their ability to transport heat radially outwards.

5 Conclusion

The investigation in this paper concerns the morphology of the flow in the area of accretion disc during tidal interaction in the binary star. Numerical methods were employed in the analysis of the gas-dynamical equations, to study the processes and resulting effects, during mass transfer between the components of the binary stars and corresponding tidal waves. We present a modeling

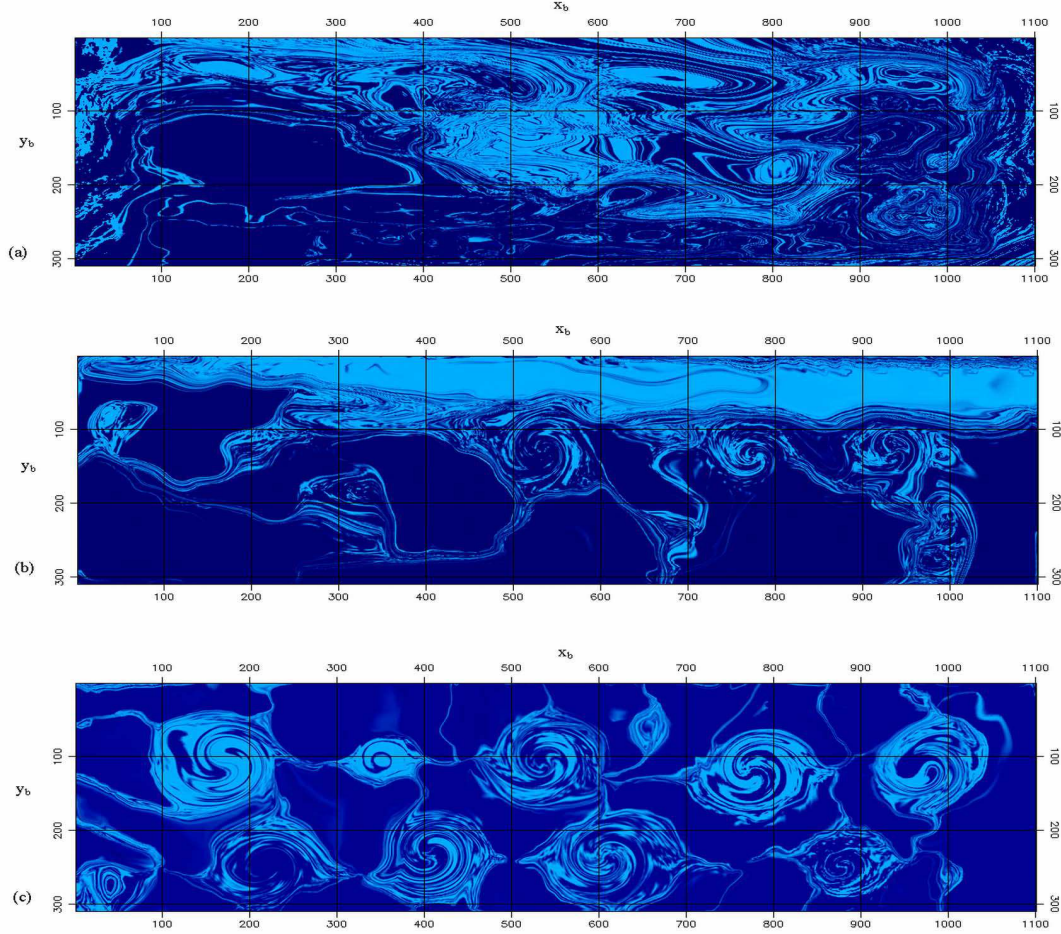


Figure 3: It is seen 3 stages of the patterns development: distortion of laminarity of the layers (a), weakly undulations (b), the final stage of structures formation in the flow (c). Each frame visualizes a covered range of about $7.687 \times 10^{-7} AU$ to $6.68 \times 10^{-7} AU$ and $7.687 \times 10^{-8} AU$ to $6.68 \times 10^{-8} AU$, referred to the boundary frame (x_b, y_b) of the calculation performance. The light Blue and dark Blue colours (light and dark in a grey scale for the printed version) show the difference in density in the interacting flow layers. The density values are increasing from dark to light zone.

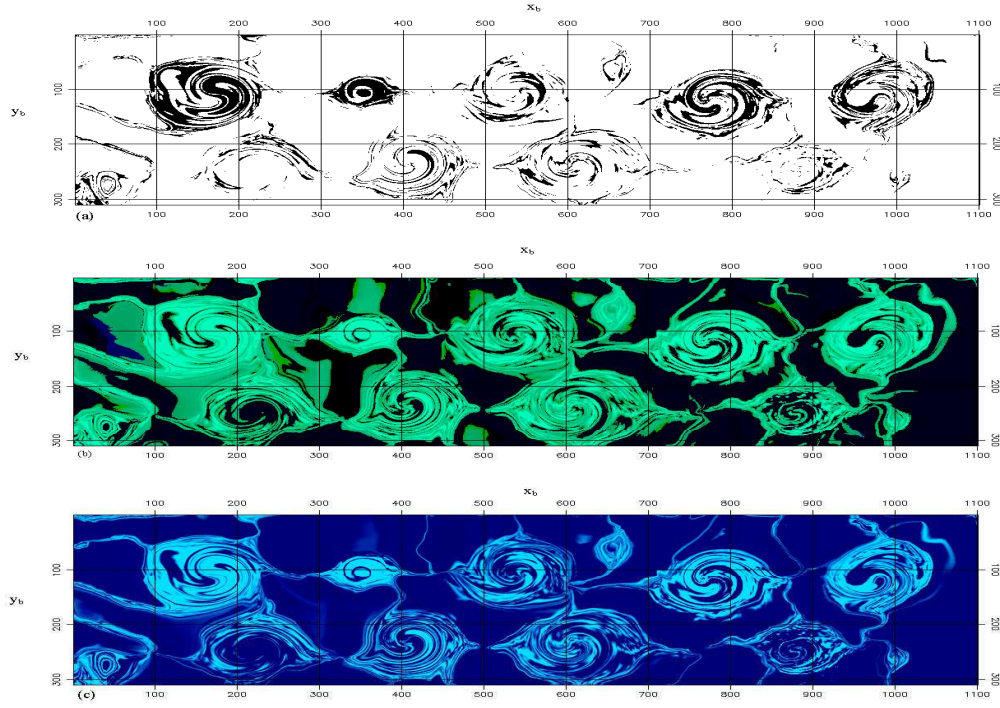


Figure 4: Processing of the vortices formation stage image: (a) Contour profile of vortices, resulting from the initial numerical simulations on the tidal flow parameters; (b) The view of such vortexes after applying the Convolution - high pass Gaussian filter; (c) The final view, after removing the data outliers from the image map.

that reveal of how the accreting flow structure could be organized after interaction processes in the binary. The change of the rate in mass transfer causes variations in the flow density, which are expressed as accumulation of matter in some places and dilution in others. This situation leads to the appearance of the 'thickened zone' that remains stable despite of the consequently tidal influences and dissipation processes. Besides the description in Sect. 2, the analysis show us that the construction of vortical transport equation (Eq. 5) is some kind of the whole disc structure's analog. It gives the relation between the angular momentum transport part (the last term in the right hand side) and describes the sources of the transport mechanism in sense of the vorticity function, and the patterns developed. In the studied interaction parts of the binary star flow, the incoming speed of flow is close to the speed of sound. Then, this tide may causes some perturbations in quantities, which changed the dynamics of the gas flow. After applying the numerical methods via numerical code the result shows the presence of two-dimensional vortical patterns. Vortices are usually local formations, but under the conditions assumed here, they could propagate globally throughout the disc. This type of vortices has often been observed in 2-D simulations of accretion discs. Vortices can be generated by two-dimensional instability as the Rossby wave instability or baroclinic instability, which have been investigated in recent years. In this study we showed once again that under the influence of tidal wave, the accretion flow could not remain stable and the conditions of patterns development are generated. Then, their movement throughout the accretion flow could support the transportation of angular momentum. The presence of a gravity-connected companion of the star can affect the physical processes in the star and appreciably change its evolution. Studying the accretion disc's structure in binary stars by using numerical methods proves that the gravitational effect of the second component may cause the appearance of spirals shocks. Tidal waves from the donor star, which usually cause a development of spiral density structure, could also be responsible for vorticity in the accretion area. However the modeling of such effects will be the topic of another report.

Appendix

We know from the perturbation analysis of Papaloizou & Pringle (1984) that in most hydrodynamical flows the flow could change its state, when some of the parameters characterizing it (e.g. the velocity, density or pressure) are perturbed. Then, the accretion flow could remain stable, become instable, turbulent, or to form a vorticity. We describe here how these perturbations are quantified and for this purpose we employ the equations of Navier-Stokes. The first step is to introduce the perturbation quantities into the parameters and to obtain an equation for hydrodynamic instability, such as:

$$V = v + u; \rho_0 = \rho + \rho'; p = P + p'; \quad (A1)$$

where V, ρ_0, p are the total quantities of velocity, density and pressure, respectively; v, ρ, P are the time averaged values; u, ρ', p' are the perturbations in time. Balbus (2003) has made a full and detailed analysis of the disc's stability, using similar expression for the perturbation function, but under different conditions of the disc flow compared to those, considered here. The perturbations are set to be in an exponent form with a power of second order and for the velocity they have the form: $u(r, \varphi) \approx u \exp(im^2\varphi - i\omega t)$. This form is applied also to the other quantities. Here ω is the wave number and m is the mode number of φ direction. For the initial values of these quantities, denoted by "zero" subscripts, we may write: $u_0(r, \varphi) \approx u \exp(Q_0)$ (we apply $Q \equiv im^2\varphi - i\omega t$), and $m_0 \approx 1, r_0 \approx 2, \varphi_0 \sim \pi, \omega t_0 \approx 3$. The second step is to express the Navier-Stokes equation

in cylindrical coordinates (r, φ, z) . The newly introduced quantities from Eq.(A1) are taken into account, which give us the form of equations transformed with perturbation values:

$$\begin{aligned} \frac{\partial V_r}{\partial t} + V_r \frac{\partial V_r}{\partial r} + \frac{V_\varphi}{r} \frac{\partial V_r}{\partial \varphi} - V_\varphi^2 r = -\frac{1}{\rho_0} \frac{\partial p}{\partial r} - \Omega \frac{\partial V_r}{\partial \varphi} + 2\Omega V_\varphi + \\ + \nu \left(\frac{\partial^2 V_r}{\partial r^2} + \frac{1}{r^2} \frac{\partial^2 V_r}{\partial \varphi^2} + \frac{1}{r} \frac{\partial V_r}{\partial r} - \frac{2}{r^2} \frac{\partial V_\varphi}{\partial \varphi} - \frac{V_r}{r^2} \right) \end{aligned} \quad (A2a)$$

$$\begin{aligned} \frac{\partial V_\varphi}{\partial t} + V_r \frac{\partial V_\varphi}{\partial r} + \frac{V_\varphi}{r} \frac{\partial V_\varphi}{\partial \varphi} - \frac{V_r V_\varphi}{r} = -\frac{1}{\rho_0 r} \frac{\partial p}{\partial \varphi} + \frac{\partial r^2}{\partial r} \Omega \frac{V_r}{r} - \Omega \frac{\partial V_\varphi}{\partial \varphi} + \\ + \nu \left(\frac{\partial^2 V_\varphi}{\partial r^2} + \frac{1}{r^2} \frac{\partial^2 V_\varphi}{\partial \varphi^2} + \frac{1}{r} \frac{\partial V_\varphi}{\partial r} - \frac{2}{r^2} \frac{\partial V_r}{\partial \varphi} - \frac{V_\varphi}{r^2} \right) \end{aligned} \quad (A2b)$$

$$\begin{aligned} \frac{\partial V_z}{\partial t} + V_r \frac{\partial V_z}{\partial r} + \frac{V_\varphi}{r} \frac{\partial V_z}{\partial \varphi} - V_z \frac{\partial V_z}{\partial z} = -\frac{1}{\rho_0} \frac{\partial p}{\partial z} + \\ + \nu \left(\frac{\partial^2 V_z}{\partial r^2} + \frac{1}{r^2} \frac{\partial^2 V_z}{\partial \varphi^2} + \frac{1}{r} \frac{\partial V_z}{\partial r} - \frac{2}{r^2} \frac{\partial V_r}{\partial z} - \frac{V_z}{r^2} \right) \end{aligned} \quad (A2c)$$

Because of the time averaging and the presence of perturbations in the quantities, some of the terms in the equations may vanish or reform their expression. The expression in z-direction brings no new information and after averaging over z, Eq. (A2c) can be ignored. The second and third term in the right hand site of Eqs. A2a and A2b, express turbulence activity. This term would allow detection of sharp changes in the instability and is called: "term of instability" (further shortly call: "inst term"). Now, following the perturbed equations (A2a, A2b), and the effect of perturbation function, next form of this "term" have been extracted: $\Omega \left(\frac{\partial r^2}{\partial r} \frac{V_r}{r} - \frac{\partial V_\varphi}{\partial \varphi} \right)$ and $2\Omega \left(\frac{1}{2} \frac{\partial V_r}{\partial \varphi} - V_\varphi \right)$. They contain the quantity of angular velocity Ω that is found to be of importance for studying the differential flow in accretion discs. It appears that the "inst term" in the above equation is significant only in r and φ directions, as should be expected in accordance with the initial conditions for this case. Then, using the mode number m from the perturbation expression we examine how the velocity and density variations develop. For the graphical visualization of the disturbances effects, we use a grid-scale measurement of values [12, 12, 12], which is more suitable to detect the results. The next initial values are applied: $V(0) = V_0$, $u(t_0) = u_0$, $t_0 \approx 1$, $r_0 \approx 1$. It results in occurrence of velocity excess during the period of disturbance (Fig. 5).

Figures 5(a-d) show how the process changes when different values of m are applied. It is observed that in a range of $(-0.2 \div -0.45)$ there is no velocity exchange. When the values of m start to decrease ($m \leq -1$) the process reverses. This leads to a fission in the solution and a suddenly drop-off in the velocity values is observed. This could be caused by some local unstable activity in the accretion discs zone (e.g. the change of mass transfer rate of the inflow matter in close binary, studied in Sect.3). The scales of the axes are constrained by the parametrization of the code.

In the next figure we show the result of applying the perturbation analysis (explained above) on the matter of interaction flow after variation in mass transfer rate. The calculations are made only for one orbital period of the rotating system. Figure 6 shows the appearing of dense pattern, called "thickened zone".

The analysis of the perturbation functions and the expression of Navier-Stokes equations presented in this Appendix help us to understand the behavior of interacting flows in close binary stars, as the processes studied in Sect.3 and 4 in the current paper.

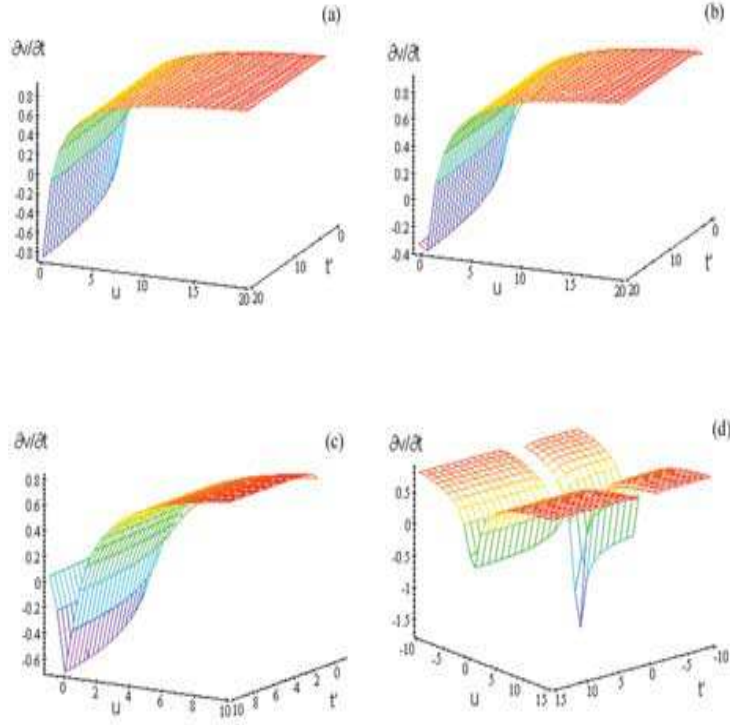


Figure 5: Velocity variations in the flow during the mass transfer. It is seen four consecutive phases that trace out the process in different values of m (Fig.5(a),5(b),5(c),5(d)). When $m \in (-0.2 \div -0.45)$ the velocity state is in a quiet (Fig. 5a). Variations start at $-0.45 > m \geq -1$ (Fig. 5b, 5c). The critical value in Fig. 5(d) is at $m = -10$, when some fission and sharply decrease of the velocity are observed.

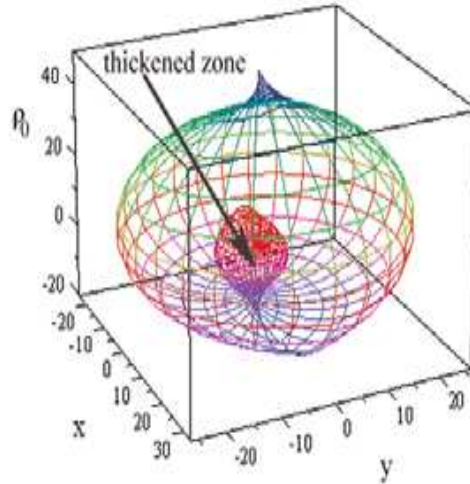


Figure 6: Thickened zone formation in the flow as a result of disturbances in the stability state, caused by mass transfer in the binary system. Calculations are for one period of time with grid $[30,30,30]$. The place of dense formation is shown with arrow.

Bibliography

- Autar, K.K., Egwu, E.K. 2008, Numerical methods with applications, 1st ed., self-publ.,
- Balbus, S. A. 2003, ARA&A, 41, 555-597
- Balbus, S. A., Hawley, J. F. 1998, Rev. of Mod. Phys, 70, 1
- Barranco, J. A. Marcus, P. S. 2005, ApJ, 623, 1157
- Bisikalo D. V., Boyarchuk A. A., Kilpio A.A., Kuznetsov O. A., 2001, Astron. Rep., 45, 676
- Bisikalo, D.V., Boyarchuk, A.A., Kaigorodov P.V., Kuznetsov O.A. 2003, Astron. Rep. 47, 809
- Boneva, D.V. 2009, Bg AJ, 11, pp. 5365
- Boneva, D.V., Filipov, L.G. 2009, Proceedings of SENS09 (International conference of Space Ecology Nanotechnology and Safety), Sofia, Bulgaria, p.360
- Boneva, D.V. 2010, BgAJ, 13, pp. 3-11, ISSN 1313-2709 (1)
- Boneva, D. 2010, AIP Conf. Proceedings, 1273,324 (2)
- Boyarchuk, A. A., Bisikalo, D. V., Kuznetsov, O. A., Chechetkin V. M. 2002, Adv. in Astron. and Astroph., Vol. 6, London: Taylor & Francis
- Bracco, A., Provenzale, A., Spiegel, E., Yecko, P. 1998, in Theory of Black Hole Accretion Disks, ed. M. Abramowicz, G. Bjornsson, J. Pringle (Cambridge: Cambridge University Press), 254
- Chang, M.J., Chow, L.C., Chang, W.S. 1991, Numerical Heat transfer, Part B, 19(1), 69-84, ISSN 1040-7790
- Clark, C., Carswell, R. 2007, Principles in Astrophysical Fluid Dynamics, Cambridge University Press, ISBN-13: 978-0-511-27379-7
- Fridman, A.M. 2007, Phys. Usp., 50, 115
- Frank, J., King, A., Raine, D. 2002, Accretion Power in Astrophysics, 3-rd edition, Cambridge University Press, New York
- Frank, J. 2008, New Astronomy Reviews, 51, 878-883
- Felder R. M., Introduction to Maple, II. Elementary Calculus and Differential Equations, North Carolina State University,
- Godon, P. 1997, ApJ, 480, 329
- Godon, P., Livio, M. 1999, ApJ, 523, 350
- Godon, P., Livio, M. 2000, ApJ, 537, 396
- Gonzalez, R., Woods, R. 1992, Digital Image Processing, Addison-Wesley Publishing Company, p 191.
- Graham, J.R. 2001, "Astronomy 202: Astrophysical Gas Dynamics". Astronomy Department, UC Berkeley
- Hairer, E., Soderling G. 2005, SIAM J. Sci. Comput., Vol. 26, 6, pp. 1838-1851
- Haddad, R.A., Akansu, A.N. 1991, IEEE Transactions on Acoustics, vol. 39, pp 723-727
- Heal, K.M., Hanse, M.L. Rickard, K.M. 1998, Maple V: Learning Guide (for Release 5), Springer, New York.
- Johnson, B. M., Gammie, C. F. 2005, ApJ, 635, 149-156 Johnson, B. M., Gammie, C. F. 2006, ApJ, 636, 63
- Klahr, H., Bodenheimer, P. 2000, Proceedings of: Discs, Planetesimals and Planets, (Astronomical Soc. Of the Pacific), vol. 219, 63
- Klahr, H., Bodenheimer P. 2003, ApJ, 582, 869-892 Klahr, H. 2004, ApJ, 606, 1070
- Lesur, G., Papaloizou, J.C.B. 2009, A&A, manuscript no. 1557
- Li, H., Colgate, S., Wendro, B., Liska, R. 2001, ApJ, 551, 874 Li, H., Finn, J., Lovelace, R., Colgate, S. 2000, ApJ, 533, 1023
- Lithwick, Y. 2007, ApJ, 670, 789L
- Lithwick, Y. 2009, Ap J, 693, 85

Lovelace, R.V.E., Li H., Colgate, S.A., Nelson, A.F. 1999, Ap.J., 513, 805-810 Monnagan, M.B., Geddes, K.O., Heal, K.M., Labhan, G., Vorkoetter, S.M. 1998, Maple V: Programming Guide, 2nd edn. (for Maple V Release 5), Springer, New York Nauta, D. 2000, Two-dimensional vortices and accretion disks, University Utrecht

Nixon, M. S., Aguado, A.S. 2008, Feature Extraction and Image Processing, Academic Press, p. 88.

Petersen, M.R., Steward, G.R., Julien K. 2007, Ap J., 658:1252-1263

Papaloizou, J. C. B., Pringle, J. E. 1984, MNRAS, 208, 721-750,

Pringle, J.E., 1985, in Interacting Binary Systems (Chapter 1), eds. J.E. Pringle, R.A. Wade, Cambridge:Cambridge University Press

Pringle, J.E. 1992, A. Note, ASP Conf. Series, 22, 14

Ritter, H. 1996, in Evolutionary Processes in Binary Stars, NATO Advanced Science Institutes (ASI) Series C, Mathematical and Physical Sciences, Vol. 477, p. 223.

Rozyczka, M., Spruit, H.C. 1993, Ap J, 417, 677

Sawada, K., Matsuda T., Hachisu I. 1986, NRAS, 219, 75

Shapiro, L. G., Stockman, G. C. 2001, Computer Vision, page 137, 150, Prentice Hall

Shen, Y., Stone, J. M., Gardiner, T. A. 2006, ApJ, 653, 513 Steeghs, D., Harlaftis, E.T., Horne, K. 1997, MNRAS, 290, L28. Shore, N.S. 2007, Astrophysical Hydrodynamics, 2-nd ed., WILEY-VCH Verlag GmbH & Co. KGaA, ISBN: 978-3-527-40669-2

Shu, F.H., (1992), The Physics of Astrophysics, Vol II: Gas Dynamics, University Science Books.

Thorne, K. 2004, Foundations of fluid dynamics, V 0415.2.K2004, <http://www.pma.caltech.edu/Courses/ph136>

Vandevenne, L., Lode's Computer Graphics Tutorial Image Filtering, Copyright (c) 2004-2007, <http://lodev.org/cgtutor/filtering.html/Convolution>